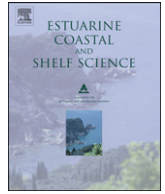


Contents lists available at [SciVerse ScienceDirect](http://www.sciencedirect.com)

## Estuarine, Coastal and Shelf Science

journal homepage: [www.elsevier.com/locate/ecss](http://www.elsevier.com/locate/ecss)

## Estuarine circulation and predicted oyster larval dispersal among a network of reserves

Amy T. Haase<sup>a,\*</sup>, David B. Eggleston<sup>a</sup>, Rick A. Luettich<sup>b</sup>, Robert J. Weaver<sup>b</sup>, Brandon J. Puckett<sup>a</sup>

<sup>a</sup>North Carolina State University, Marine, Earth and Atmospheric Sciences, Campus Box 8208, Raleigh NC 27695, USA

<sup>b</sup>University of North Carolina, Institute of Marine Sciences, 150 Coker Hall, 3431 Arendell Street, Morehead City, NC 28557, USA

### ARTICLE INFO

#### Article history:

Received 14 June 2011

Accepted 14 February 2012

Available online xxx

#### Keywords:

larval dispersal  
connectivity  
oyster restoration  
surface drifters  
hydrodynamic model  
Pamlico sound  
marine reserves

### ABSTRACT

A critical component to understanding connectivity of isolated populations of marine organisms (i.e., metapopulations) is quantifying hydrodynamic paths of dispersal, and variation in the strength of these hydrodynamic connections. We replicated 3-dimensional wind-driven circulation patterns in Pamlico Sound (PS), North Carolina, USA using a numerical hydrodynamic model (ADCIRC, ADvanced CIRCulation) in conjunction with a particle-tracking model (PTM) to predict larval dispersal of the eastern oyster (*Crassostrea virginica*) and estimate connectivity among a network of ten no-take oyster broodstock reserves in PS to inform restoration efforts. ADCIRC was forced with wind observations, which were predominately southwesterly during May–November 2007 when oyster larvae were dispersing in PS. Acoustic Doppler Current Profilers and surface drifters were used to validate ADCIRC-predicted current velocities and PTM-predicted larval dispersal, respectively. ADCIRC reliably predicted current velocities at different locations in PS, especially currents near-surface ( $R = 0.6$ , lags  $< 2$  h). The PTM accurately predicted ( $R > 0.5$ ) the total and net distance transported by drifters, which ranged from 1 to 63 km and 0.3–42 km, respectively over  $\leq 7$  days. Potential oyster larval connectivity was not uniform among broodstock reserves in PS. Of the 100 possible connections, 24 were present. Eight of the 10 reserves provided  $\geq$  one inter-reserve connection, with 4 being the most. Self-recruitment occurred at all but one reserve. Spatial variation in the degree of potential oyster larval connectivity in PS, combined with evidence for spatiotemporal dynamics of oyster populations, provides strong evidence for an oyster metapopulation and possibly source-sink dynamics within the network of no-take reserves.

Published by Elsevier Ltd.

### 1. Introduction

A fundamental issue concerning recruitment dynamics of marine organisms and marine conservation biology involves identifying the paths of dispersal connecting isolated populations, and how spatiotemporal variation in the intensity of dispersal along these paths influences population connectivity, the successful exchange of individuals among isolated populations, and, ultimately, population dynamics (Cowen et al., 2007; Cowen and Sponaugle, 2009 and references therein). Most benthic marine organisms have limited mobility as adults such that dispersal, the transport and spread of larvae from natal origin over the pelagic larval duration, connects geographically isolated populations that

often vary in their demographic rates, forming a metapopulation (Levins, 1969; Hanski, 1998). Due to asymmetrical population connectivity and variation in demographic rates, subpopulations within a metapopulation can be classified as sources, which contribute more births than deaths to the metapopulation, or sinks if the opposite is true (Figueira and Crowder, 2006; Lipcius et al., 2008).

Our understanding of marine population connectivity is generally considered rudimentary (Cowen et al., 2006; Steneck, 2006; Becker et al., 2007). Cowen and Sponaugle (2009) identified several challenges to improving our understanding of connectivity, three of which we address herein: (1) observations – determination of spatial scales of connectivity, (2) explanations – mechanisms underlying dispersal and connectivity, and (3) applications – issues of conservation and resource management. Several methods, including hydrodynamic modeling, geochemical and genetic markers, and drifters have been used to estimate dispersal and connectivity (Cowen et al., 2006; Becker et al., 2007; Hare and Walsh, 2007; Cudney-Bueno et al., 2009; Fodrie et al., 2011). Each

\* Corresponding author.

E-mail address: [amy.haase@noaa.gov](mailto:amy.haase@noaa.gov) (A.T. Haase).

<sup>1</sup> Present address: NOAA, 1325 East-West Hwy, SSMC-2/10440, Silver Spring, MD 20910 USA.

method, however, has limitations. For instance, bio-physical models need rigorous empirical validation using geochemical markers or drifters, each of which are potentially constrained by spatial resolution and restricted dispersion compared to small larvae whose dispersal can be greatly influenced by diffusion (North et al., 2008; Cowen and Sponaugle, 2009). Consequently, integration of multiple methods and rigorous validation are required to enhance our ability to successfully predict larval dispersal and connectivity. In this study, we utilized a hydrodynamic modeling approach in conjunction with a particle-tracking model, each validated with Acoustic Doppler Current Profilers and surface drifters, respectively, to estimate dispersal patterns and potential larval connectivity of eastern oysters (*Crassostrea virginica*) within an estuarine network of no-take oyster broodstock reserves.

In marine systems, the protection, restoration, and management of species, including oysters, increasingly involves the establishment of no-take reserves closed to harvest (Briers, 2002; Spalding et al., 2008; Powers et al., 2009; Schulte et al., 2009). Reserve networks have been promoted as a viable solution because the boundaries of a single reserve are often much smaller than the protected species' geographic range and larval dispersal distance (Roberts et al., 2003). For isolated reserves to function as a network, inter-reserve connectivity is required and, thus, knowledge of larval dispersal and connectivity within the network is vital for informing management and restoration efforts (Gaines et al., 2010).

### 1.1. Study species

The eastern oyster is an economically and ecologically important species that inhabits estuarine and coastal waters from the Gulf of St. Lawrence to the Gulf of Mexico and West Indies (Stanley and Sellers, 1986; Beck et al., 2011 and references therein). Oysters are protandrous hermaphrodites, initially maturing as males several months post-settlement, and transitioning to functional females at ~40 mm shell height (Burkenroad, 1931; Mroch, 2009). In Pamlico Sound (PS), North Carolina, USA, oyster spawning occurs from May to October with fecundity and settlement peaks during May (Mroch, 2009) and June (Eggleston and Puckett, unpublished data), respectively. A smaller, secondary settlement peak typically occurs in July/August. Gametes are freely spawned into the water column where fertilized eggs develop into dispersing larvae with a pelagic duration of ~14–25 days depending on water temperatures, salinity, turbidity, oxygen content and available nutrients (Deksheniaks et al., 1993, 1996).

The overall objectives of this study were to (1) assess the efficacy of 2-dimensional (2D) versus 3-dimensional (3D) ADCIRC (ADVanced CIRCulation) hydrodynamic models in predicting current velocities in PS by validating predictions with Acoustic Doppler Current Profilers, (2) couple a Particle-Tracking Model (PTM) to ADCIRC to predict oyster larval dispersal under observed winds, and validate predicted dispersal paths using surface drifters, and (3) use the information from objectives (1) and (2) to estimate potential oyster larval settlement areas and population connectivity among oyster broodstock reserves in PS.

## 2. Methods

### 2.1. Study system

Pamlico Sound, the largest water body of the Croatan-Albemarle-Pamlico-Estuarine System (CAPES), is located in the eastern coastal region of North Carolina, USA and sheltered from the Atlantic Ocean by a grouping of barrier islands known as the 'Outer Banks' (Fig. 1). Connections to the Atlantic Ocean are limited

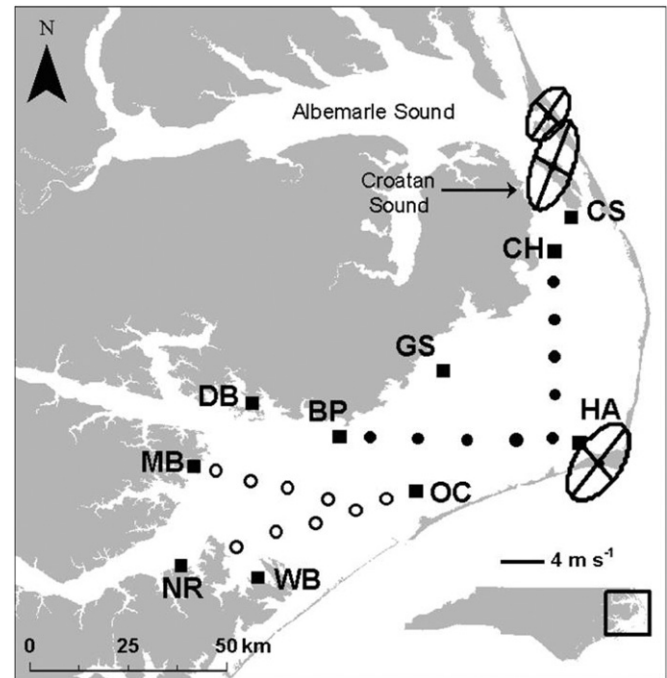


**Fig. 1.** Map of the Croatan-Albemarle-Pamlico-Estuarine System (CAPES). Location of oyster reserves in Pamlico Sound are depicted by closed squares (not to scale). Acoustic Doppler Current Profilers were deployed at CH and OC reserves. Circles represent drifter release locations for the northern (closed) and southern (open) basins of Pamlico Sound. Principal axes of variance of hourly wind velocities from May to November 2007 are shown for meteorological stations listed north to south at Kill Devil Hills (KFFA), Manteo (KMQJ), and Hatteras (KHSE). CS, Croatan Sound; CH, Crab Hole; GS, Gibbs Shoal; BP, Bluff Point; DB, Deep Bay; MB, Middle Bay; NR, Neuse River; WB, West Bay; OC, Ocracoke; HA, Hatteras. Scale bars depicting wind velocity and distance as well as map of North Carolina are inset for reference.

to four narrow inlets (Lin et al., 2007). Circulation is dominated by wind-driven currents and freshwater input (Pietrafesa and Janowitz, 1988; Luettich et al., 2002), with little evidence of strong vertical shear flows at different locations in PS (this study). Average depth in PS is 4–5 m with the deepest basin only 7–8 m (Pietrafesa and Janowitz, 1988). Wind forcing is highly variable, changing velocity at hourly to daily intervals, but does sustain regular seasonal patterns with winds predominately southwesterly in the late-spring/summer and northeasterly in late-summer/fall (Xie and Eggleston, 1999; Eggleston et al., 2010). Since oyster larval dispersal is primarily driven by horizontal currents, knowledge of these currents is important to explaining the mechanisms underlying dispersal and connectivity.

### 2.2. Numerical hydrodynamic model

We used both the 2D and 3D ADCIRC, a non-linear finite-element hydrodynamic model (Luettich et al., 1992; Reynolds-Fleming, and Luettich, 2004; Reyns et al., 2006, 2007), in conjunction with a particle-tracking model to predict currents and simulate oyster larval dispersal in PS. ADCIRC solves the governing equations of motion which are formulated using the traditional hydrostatic pressure and Boussinesq approximations. Momentum equations in the 2D and 3D form are used to obtain velocity solutions (Luettich and Westerink, 2004). ADCIRC has produced vector fields that are in good agreement with observed currents in the Neuse River Estuary located in the southwestern portion of PS (Luettich et al., 2002), as well as in the northern basin of PS (Reyns et al., 2006, 2007). To further validate ADCIRC, we collected Eulerian and Lagrangian observations of current velocities throughout PS.

We used a triangular model grid developed by Reynolds et al. (2006, 2007) for the entire CAPES that contained 22,425 nodes and 41,330 elements in the horizontal (Fig. 2). This unstructured grid contained a nodal spacing range of 300 m near inlets and adjacent river estuaries to 1 km in the main body of PS. In the vertical, both a single layer (i.e. 2D) and seven variable depth layers (i.e. 3D) were selected to resolve the vector field. Parameter settings used by Reynolds et al. (2006, 2007), such as slip (bottom friction) and drag coefficients, bottom roughness, turbulence closure, and length of time steps provided an initial set-up for model runs and were modified iteratively based on success of the model run in reproducing observations of current velocities. Coriolis force was neglected in the model runs because the characteristic time scale of motion in our small domain was less than a day, the minimum required for Coriolis acceleration to noticeably affect current velocities (Luettich et al., 2002). Two scales of current velocities were generated: (1) "Station velocities", which were velocities at all depths from a single model grid node (the equivalent of time-series data collected from a unique geographic location), and (2) "Global velocities", which were velocities from all model grid nodes for the entire domain at all depths to produce a 3D vector field. Global and station velocities were produced at hourly time steps. Geographic coordinates and output time intervals of these stations were selected to match the locations where Eulerian observations were collected via moored ADCPs (Fig. 1).

### 2.3. Particle-tracking model

Global velocities were formatted for use with a particle-tracking model (PTM) which required input from a single water depth and were constrained in the horizontal plain. The PTM was designed to

be used in conjunction with files from the ADCIRC model, including grids and global velocities. The single water depth that best matched the observations collected by the ADCP was selected to force the PTM. This method was valid since observed vertical velocity profiles contained very little shear (see 3.1 2D versus 3D ADCIRC validation). Specifications of the predicted particle tracks were written in a parameter file that included: start time, duration, number of time-steps, and number and initial locations of particles to be tracked. Particles simulated in the PTM were numerically advected to new locations with each time step based on velocities at surrounding model grid nodes. For each particle released at each time step, the PTM output contained unique particle numbers, as well as latitude and longitude position reports.

### 2.4. Meteorological observations and model forcing

Hourly wind observations were obtained from the National Weather Service (NWS) for the period May to November, 2007 for three stations: Cape Hatteras (Fig. 1), Kill Devil Hills, and Manteo, NC. These wind observations encompassed the active spawning period of oysters in PS (Mroch, 2009; Eggleston and Puckett, unpublished data). Cross-correlations, principal component analysis (PCA), and calculation of monthly mean wind velocities were performed to determine spatial variation in the wind field over PS. The major axis of variation in velocities at all three stations was oriented along the northeast–southwest axis of PS (Fig. 1). Cross-correlation coefficients between wind velocities measured at Hatteras and the other wind stations ranged from 0.75 to 0.85 with lags ranging from 0 to 3 h. Winds were spatially coherent in PS and wind observations at Hatteras formed the most complete dataset out of three possible meteorological stations, therefore wind data from this station was used to force the numerical ADCIRC model. Mean wind velocity arrows were directed east of north at Hatteras, indicating predominant southwesterly wind during the oyster spawning season.

### 2.5. Hydrological observations and instrumentation

Predicted vector fields produced by the 2D and the 3D ADCIRC models, as well as simulated trajectories from the PTM, were correlated with Eulerian and Lagrangian velocity observations collected in PS via two types of instruments: (i) moored Acoustic Doppler Current Profilers (ADCPs), and (ii) surface drifters.

#### 2.5.1. Acoustic Doppler Current Profilers

Two RD Instrument ADCPs were placed on the seafloor in each of two oyster broodstock reserves (Crab Hole and Ocracoke) in PS during late spring to early fall of 2007 (Fig. 1). The ADCPs were fastened to the base of aluminum frames at depths of 4–6 m and programmed to sample currents every 10 min for 180 days. Depth of each bin (sample volume as a function of range of the instrument), which determines the vertical resolution of data collection, was set to 0.2 m with 30 bins. This arrangement yielded a total depth of data collection at 6 m. The deepest half meter and surface half meter were not sampled because of instrument limitations.

Cross-correlation analyses were used to determine the efficacy of 2D versus 3D ADCIRC hydrodynamic models by testing the relationship between observed versus predicted depth-specific station velocities at Crab Hole and Ocracoke. The ADCP bin nearest to the ADCIRC variable depth layer was used for comparisons. Cross-correlations identified the lead or lag between predicted and observed hourly-averaged east-west (U) and north-south (V) velocity components from the ADCPs with correspondent station velocity output from the ADCIRC model. The ADCP bin nearest to

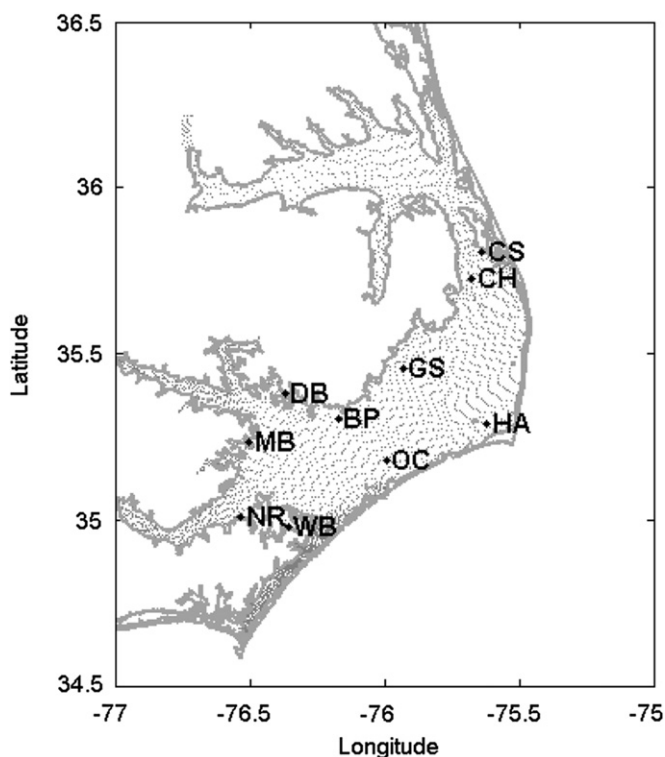


**Fig. 2.** Map of Pamlico Sound oyster reserves and ADvanced CIRculation (ADCIRC) model grid nodes. Oyster reserve names are abbreviated: Croatan Sound (CS), Crab Hole (CH), Gibbs Shoal (GS), Bluff Point (BP), Deep Bay (DB), Middle Bay (MB), Neuse River (NR), West Bay (WB), Ocracoke (OC) and Hatteras (HA). Every 5th model grid node was plotted to enhance readability.

the ADCIRC variable depth layer was used for comparisons. Additionally, PCA and calculation of monthly mean velocities were performed on the ADCP data to determine the mean flow at these two oyster reserves.

### 2.5.2. Surface drifters

Microstar surface drifters (herein “drifters”) built by Pacific Gyre were deployed in PS from May to September, 2007. Drifters consisted of spherical plastic cases that provided buoyancy and housed batteries (8–10 day life with settings below), a temperature sensor, and a GPS sensor with an antenna. Each drifter consisted of four drag-producing triangular nylon sails extending radially the entire length of a negatively buoyant polyvinyl chloride (PVC) tube centered at 1 m water depth and tethered by a nylon cord to the spherical case. Four horizontal tubes connected at a central joint supported the vertical sails. Drifters were programmed to record their location determined by the onboard GPS sensor every 10 min, with three reports containing the following information transmitted every 30 min: locations, sea surface temperatures, and time of observations. Up to 144 position reports were recorded each day making re-capture and re-deployment in the field possible.

During the summer of 2007, 17 drifter releases were conducted with 1–5 drifters per release (Table 1). A collection of concurrently released drifters is referred to hereafter as a “batch”. Over a 13-week period, four to nine drifters and up to two batches were deployed simultaneously and allowed to drift for up to one week along transects between oyster reserves within PS (Fig. 1). Drifter deployment batch #s 21–29 were released into the northern portion of PS, and batch #s 31–36 released into the southern portion of PS (Table 1).

Several challenges were encountered when deploying drifters. These instruments ran aground in depths less than 1.5 m, which in PS includes large areas near the shoreline and over shoals. Drifters that ran aground were identified by notes in a log made at the time of retrieval, plotted position reports, and zero velocity values. Drifter records of groundings were truncated by distance-differencing between position reports. For example, if the total change in position of each report was less than the accuracy of the GPS (<10 m) for the latter part of a record, it was deleted. In

addition to running aground, there were several instances where drifters detached from their drogues, which was evident during retrieval and in the data when drifter velocities more than doubled within a single time-series. These data were also eliminated from analyses. Other instances where data were truncated included: (i) erroneous position reports, such as those several kilometers outside the study area or on land, (ii) reports separated by more than 12 h, which were indicative of GPS signal loss, and (iii) duplicate reports. Temporal and spatial variation in drifter velocity cannot be treated with low-pass filters to remove inertial or tidal oscillations because the records are too short—tidal oscillations occur on a semi-diurnal and diurnal time scale. Currents within the study area, however, are not driven primarily by tides but by winds (see 2.1 Study system); therefore the lack of filtering did not create a problem in analyzing data. Various drifter metrics, such as total and net distance traveled, were generated.

### 2.6. Oyster larval dispersal and connectivity

Predicted oyster larval dispersal from ten oyster broodstock reserves in PS (Fig. 1), were generated using the PTM driven by the 3D ADCIRC global velocity fields to assess potential larval connectivity among reserves. Dispersal of particles (i.e., virtual larvae) was modeled as non-swimming larvae near the surface. Particles were released from five initial starting locations within each of 10 oyster reserves in PS, one at each of the four corners and one in the center of each reserve, and allowed to “drift” for 14–21 days.

The relatively small spatial footprint of reserves (<1 km<sup>2</sup>) relative to the model grid cells (300 m<sup>-1</sup> km), combined with the PTM limitation of no turbulent diffusion (North et al., 2008) resulted in all model particles following a single trajectory/path during a 14 d trial simulation conducted at each reserve. Therefore, an alternate simulation scenario was adopted to overcome the omission of turbulent processes in the PTM and to artificially force particles to diffuse. First, the initial starting locations were expanded from a single point to a ‘five dice’ pattern (following the method used with drifters by Doble and Wadhams, 2006) in or near each of the ten oyster reserve boundaries. The starting locations were then incrementally moved away from reserve corners at incremental distances of 0.01° latitude/longitude until independent transport paths were produced. All final particle release locations were about 0.03° from the center of a given reserve and located in separate model grid cells. Second, particles were released at 24 h intervals over 26 daily iterations starting each day from May 28–June 10, 2007 and from June 20–July 11, 2007. Each iteration was dispersed for 21 d to simulate a typical pelagic duration of oyster larvae. These simulations were set to correspond to the primary (May 28 to June 10) and secondary (June 20 to July 11) oyster settlement peaks observed annually in PS (see 1.1 Study species) and also coincided with drifter deployment dates. These dates also allowed for ample spin-up time for the ADCIRC model (28 d). A total of 50 particles were released, 5 from each of 10 reserves. Oyster larvae become competent to settle at 14 d (North et al., 2008), thus figures were created by plotting the last 7 d of particle paths (i.e., days 15–21) for each of the iterations according to their oyster sanctuary of release. Areas in which simulated oyster larvae traveled between day 15 and 21 of modeled dispersal were referred to as “potential settlement areas”. Potential settlement areas for particles from a given reserve were qualitatively compared to one another in terms of general size, shape and overall extent. Quantitative measures are described below.

We examined three aspects of potential larval connectivity—whether or not (i) larvae dispersed from one reserve to another, (ii) larvae dispersed to their natal reserve, and (iii) how increasing the footprint of a given reserve altered (i) and (ii). A connectivity

**Table 1**

Summary of drifter batch releases. Deployment locations are identified by an abbreviation of the oyster reserve name or nearby landmark: Crab Hole (CH), Bluff Point (BP), Hatteras (HA), Middle Bay (MB), Neuse River (NR), Ocracoke (OC), and (see Figs. 1 and 2 for locations). Wind conditions were recorded at time of release while on site. Batch numbers in parentheses occurred simultaneously with batch number listed. Wind directions are listed by meteorological convention (i.e. s = southerly, n = northerly, etc.). Batches used in comparison to the PTM are bolded.

Batch No.	Date deployed	No. of drifters	No. of days	Location	Wind (m/s)
21	11-May-2007	4	5	CH	s 2–4
<b>22</b>	<b>29-May-2007</b>	<b>4</b>	<b>3</b>	<b>CH–HA</b>	<b>n 2–4</b>
<b>23 (32)</b>	<b>12-Jun-2007</b>	<b>4</b>	<b>3</b>	<b>CH–HA</b>	<b>nw 2–4, ne 7–9</b>
<b>24</b>	<b>18-Jun-2007</b>	<b>4</b>	<b>4</b>	<b>BP–HA</b>	<b>sw 2–4</b>
<b>25 (33)</b>	<b>25-Jun-07</b>	<b>4</b>	<b>4</b>	<b>BP–HA</b>	<b>se 2–4</b>
26 (34)	16-Jul-2007	4	3	BP–HA	sw 4–9
27 (35)	23-Jul-2007	4	4	CH–HA	n 9
28 (36)	30-Jul-2007	4	4	BP–OC	e 2–4
29	12-Sep-2007	4	2	CH	nne 7
31	21-May-2007	5	4	NR–OC	ne 2–4
<b>32</b>	<b>11-Jun-2007</b>	<b>5</b>	<b>4</b>	<b>MB–OC</b>	<b>nw 2–4, ne 7–9</b>
<b>33</b>	<b>26-Jun-2007</b>	<b>4</b>	<b>3</b>	<b>NR–OC</b>	<b>s 2–7</b>
34	17-Jul-2007	4	3	NR–OC	sw 4–9
35	24-Jul-2007	5	3	NR–OC	n 9
36	30-Jul-2007	4	4	NR–OC	e 2–4
37	7-Aug-2007	4	4	NR–OC	sw 2–4
38	13-Aug-2007	2	7, 10	NR–OC	s 2

matrix, whereby rows represent the natal reserve and columns represent the settlement reserve, were generated by visual inspection of predicted larval dispersal. If a particle traveled from one reserve to another, these reserves were considered biologically connected via larval dispersal. If a particle returned to its natal reserve, that reserve was deemed self-recruiting. Connectivity scores of 10 were given to particles that either dispersed from one reserve to within the borders of another reserve or self-recruited. We also simulated the effects of increasing reserve size on connectivity by expanding reserve boundaries by 0.01°, 0.02°, and 0.03° (about 1 km, 2 km, and 3 km respectively), whereby connectivity was scored as a 9, 8, and 7, respectively. Reserve connectivity was calculated by summing the scores in each row (i.e., each individual reserve connection equals a maximum of 10 for a total score of 100 should it be connected to all reserves). For example, if particles released from one reserve returned to the natal reserve and nine additional tracks from the natal reserve entered the borders of the other nine reserves, this set of 10 tracks would add-up to 100.

### 3. Results

#### 3.1. 2D vs. 3D ADCIRC validation

Initial parameter settings for the 2D and 3D ADCIRC models generated output values that correlated poorly (average  $R < 0.4$  with lags up to 98 h) with observations of velocities both with and without tidal frequencies. Parameter settings were subsequently modified incrementally, for instance modifying slip coefficient values from 0.005 to 0.0025 by increments of 0.0005, until optimum correlation values were reached. A total of 30 model runs were conducted that resulted in final parameter settings that were then used to generate global velocity output for two time-periods: May 1 to July 14, 2007 and July 15 to September 15, 2007. These two

time-periods were selected to encompass surface drifter deployment dates (see below) and peak spawning periods for oysters in PS (Eggleston and Puckett, unpublished data). Splitting the output into two time-periods also enhanced processing efficiency.

In general, there was good agreement for both time-periods between observed current velocities measured with ADCPs and velocities predicted with the 3D ADCIRC model, but not with the 2D model. Predicted flow velocities were similar to, though lower in magnitude, than observed velocities (Figs. 3–5). Predicted currents from both 2D (not shown) and 3D models were correlated with wind forcing (Fig. 5). Comparing current velocity components at both sites in PS, the strongest correlations between observed and predicted currents were found at Ocracoke in the U-component and Crab Hole in the V-component (Fig. 5). Within a given site, correlations were strongest between observed and predicted near-surface versus deeper currents, with highest correlation coefficients of nearly 0.6 at both Ocracoke and Crab Hole (Fig. 5) at lags  $< 2$  h. Predicted currents replicated changes in magnitude and direction of observed currents within each depth-specific velocity on a daily and weekly time scale, but did not recreate the higher magnitude velocity oscillations operating on hourly time-scales. Predicted velocities peaked near the water surface at a speed of  $\sim 0.5$  m/s and decreased to  $\sim$  zero near-bottom. Conversely, observed velocities were more homogenous across water depths, with relatively little evidence of strong vertical shear. For example, observed velocities near the bottom of PS were nearly as strong at mid-depth as they were at the surface (both  $\sim 0.2$  m/s). Removing tidal constituents from the ADCP velocities lowered the correlations between observed and predicted velocities ( $R$  decreased by  $\sim 0.02$ ). Tidal-forcing was visible in the U-component of the observations at Ocracoke, as indicated by periodic oscillations matching those of only M2 and P1 tides; however, the model forcing did not include tides, and as expected, was not replicated. Based on the better fit of the 3D versus 2D ADCIRC-predicted

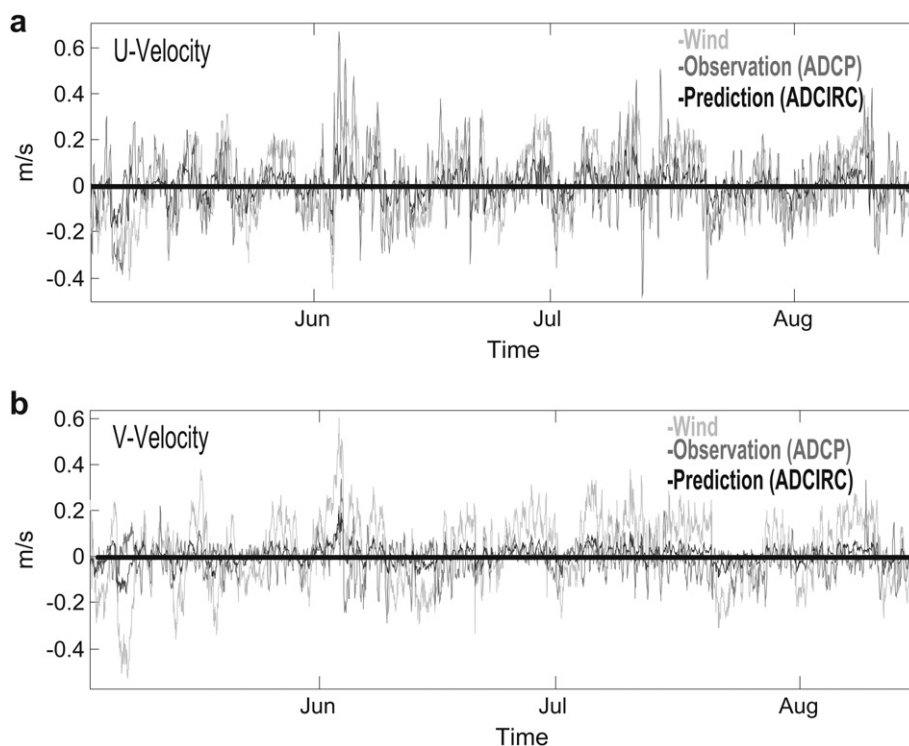


**Fig. 3.** Comparison of observed (black) and 3D ADCIRC-predicted (dark gray) surface velocities in the a) U (east-west) and b) V (north-south) directions at the Ocracoke oyster reserve with winds measured at Cape Hatteras (light gray) overlaid. Wind velocities were an order of magnitude greater than observed and predicted currents, therefore, to fit within the same plot only 20% of the magnitude of the wind velocity is shown.

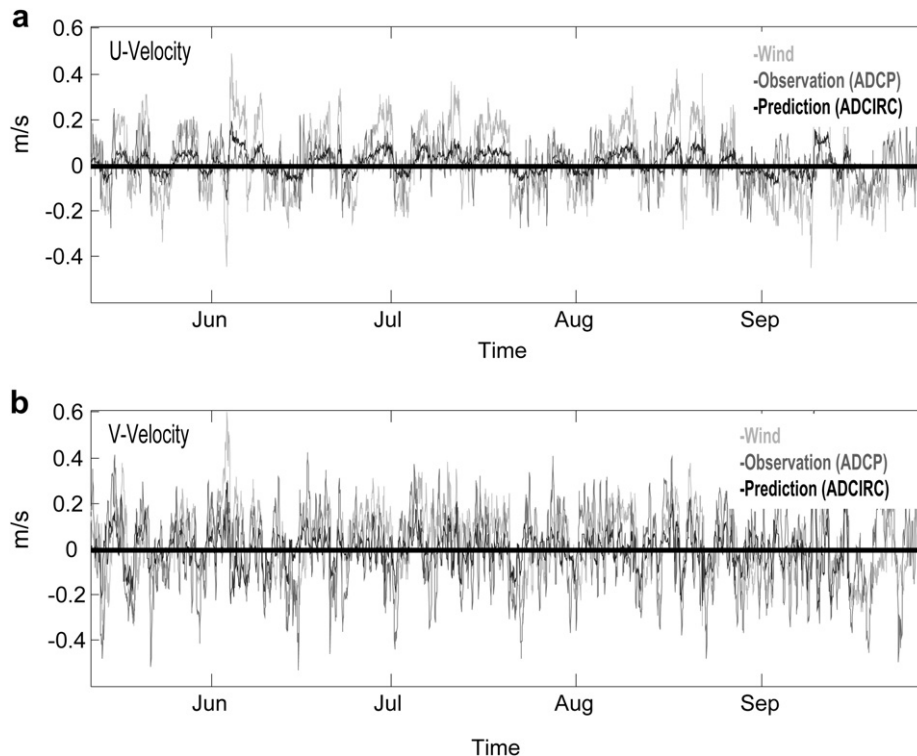


**Fig. 4.** Comparison of observed (black) and 3D ADCIRC-predicted (dark gray) surface velocities in the a) U (east-west) and b) V (north-south) directions at the Crab Hole oyster reserve with winds measured at Cape Hatteras (light gray) overlaid. Wind velocities were an order of magnitude greater than observed and predicted currents, therefore, to fit within the same plot only 20% of the magnitude of the wind velocity is shown.

currents and ADCP-based observed currents, the 3D ADCIRC hydrodynamic model was used to predict oyster larval dispersal.

### 3.2. PTM validation using drifters

PTM driven by vector fields produced by the ADCIRC model were validated by the drifters. Twenty-five drifter deployments (deployment batch #s: 22–25, 32 and 33; Table 1) were selected to validate the PTM based on date of deployment (i.e., peak oyster

spawning) and duration (i.e., >70 h). All 10-min drifter reports were hourly-averaged to create a consistent time interval with hourly output from the PTM, and to fill in short (<2 h) data gaps. Predicted drifter paths were simulated by entering the following data into the PTM parameter file: initial deployment time, duration, and drifter release locations, and number of drifters for each deployment batch. Particle dispersal (i.e., latitudes and longitudes) predicted by the PTM was highly correlated with observed surface drifter paths (Table 2; Fig. 6), with an overall correlation coefficient of 0.77 for longitude and 0.73 for latitude; 11 of 21 possible correlations produced coefficients greater than 0.9 (Table 2). Correlations tended to be highest in areas with the greatest velocities that were produced by either strong wind velocities or by geographic location. For example, drifters deployed in near-shore environments and that traveled along the major northeast/southwest axis of PS (e.g., drifter batch #25, Table 2) had the highest correlation between predicted and observed latitude (Table 2).

Total and net distances transported (difference between the release and retrieval location) were calculated and compared for both observed drifter paths and modeled particle dispersal paths. Total distances transported were calculated by summing the individual changes in position at each time step (predicted) or report (observed). The net distance transported was calculated by taking the difference in drifter recovery site with the drifter launch site for both observations and predictions. The selected observed drifter paths were then (i) qualitatively compared to those predicted by the PTM by plotting each on the same figure, and (ii) quantitatively compared by cross-correlations between the observed and predicted latitude and longitude to the precision of hundredths of seconds. Predicted total distances were highly correlated ( $R > 0.65$ ) with observed distances, with correlation coefficients increasing with distance transported. Predicted total distances from the PTM, however, were generally 10% greater than total distance

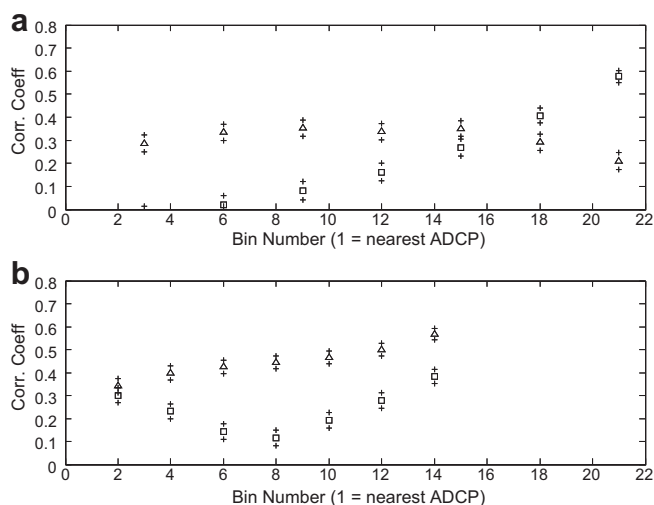


**Fig. 5.** Cross-correlation coefficients between depth-specific observed and predicted current velocities in the U (east-west; squares) and V (north-south; triangles) direction, with upper and lower limits (plus symbols) at a) Ocracoke and b) Crab Hole oyster reserves.

**Table 2**

Summary of total and net transport of observed drifter and modeled particle paths, and cross-correlation coefficients by drifter deployment batch. Distances are in kilometers. See Methods: Drifter validation of PTM and predicted oyster larval dispersal for summary statistic calculations. Deployments containing insufficient data for statistical correlations are shown by NED due to instrument failure and error in data collection.

Deployment batch No.	Surface drift buoy			Model			Comparison		
	Number of Obs.	Total distance (km)	Net transport (km)	Total distance (km)	Net transport (km)	Difference in Endpoints (km)	R longitude	R latitude	Mean R
DB22	145	17.93	16.45	21.11	7.10	9.92	0.86	0.39	0.63
	151	20.67	6.74	27.47	5.59	5.37	0.94	0.88	0.91
	67	14.59	4.96	19.72	5.70	5.46	NED	NED	NED
	136	9.59	8.38	33.95	9.84	4.22	0.798	0.814	0.81
DB23	149	31.10	25.87	39.61	29.85	4.67	0.98	0.98	0.98
	114	26.91	24.45	34.94	29.22	8.35	0.98	0.99	0.99
	25	14.30	13.34	28.49	19.53	10.68	NED	NED	NED
	65	20.78	13.82	22.00	14.40	6.06	0.93	0.95	0.94
DB32	184	1.04	0.90	5.08	0.33	0.91	-0.08	-0.08	-0.08
	167	32.67	18.18	32.86	25.12	13.47	0.81	0.88	0.85
	176	31.28	14.70	38.77	27.24	15.70	0.98	0.64	0.81
	141	46.21	25.22	57.21	25.80	1.03	0.954	0.943	0.95
DB24	126	51.56	27.49	54.13	33.07	5.80	0.975	0.972	0.97
	190	53.97	4.75	33.56	12.99	8.78	NED	NED	NED
	179	46.77	21.94	58.07	29.10	8.51	0.964	0.964	0.96
	188	62.67	20.04	54.72	28.72	12.77	0.966	0.436	0.70
DB25	121	46.76	8.56	34.42	9.57	5.58	0.498	0.498	0.50
	174	46.70	42.24	9.86	4.00	40.27	NED	NED	NED
	170	29.27	26.04	41.33	35.80	9.15	0.94	0.99	0.97
	180	19.88	16.46	24.18	16.92	4.58	0.838	0.988	0.91
DB33	101	30.14	22.75	30.33	22.21	4.69	0.96	0.82	0.89
	114	30.77	26.05	36.07	32.45	6.25	0.89	0.95	0.92
	113	21.61	14.41	36.96	33.47	19.83	0.95	0.94	0.95
	73	22.97	3.74	29.29	21.84	25.14	-0.56	-0.62	-0.59
82	15.91	3.43	20.12	15.77	14.01	0.53	0.94	0.74	

transported by the drifters. Predicted and observed total distances ranged from 5 to 58 km and 1–63 km, respectively (Table 2). Similar to predictions of total transport, predicted net transport was 20% greater than observed net transport ( $R = 0.5$ ), which ranged from 0.3 to 35.8 km and 0.9–42.2 km, respectively (Table 2).

### 3.3. Oyster larval dispersal and connectivity

#### 3.3.1. Potential settlement areas

Initial release location of particles influenced both the spread and distance traveled of virtual particles over a 14–21 d dispersal period (Fig. 7). Numerous particle paths terminated in the center of the northern basin of PS, or along the shoreline, such as those originating from Gibbs Shoal, Bluff Point, and Ocracoke (Fig. 7c, d and i). Particles released from the Neuse River and West Bay along the southern shore of PS traveled the greatest distances (~110 km) to Oregon Inlet near Croatan Sound in the north, crossing the entire sound along the western shore (Fig. 7g and h). Particles released at Ocracoke spread throughout the northern basin of PS, whereas particles released from Hatteras remained near the eastern shore until they traveled a significant distance north (Fig. 7i and j).

Qualitatively, the area of PS that served as potential settlement areas for virtual oyster larvae varied according to the location of the natal reserve. For example, the largest potential settlement areas, filling two-thirds of PS, corresponded to virtual larvae released from Gibbs Shoal and Bluff Point (Fig. 7c and d), both located on the western shore of PS. Conversely, the smallest potential settlement areas corresponded to virtual larvae released at Deep Bay and Middle Bay (Fig. 7e and f), both near the mouth of the Pamlico River. Virtual larvae released from the northern most reserves, Croatan Sound and Crab Hole, were exported to Albemarle Sound (Fig. 7a and b), where salinities are likely too low for survival of oyster larvae (Deksheniaks et al., 1993; Xie and Eggleston, 1999). Potential

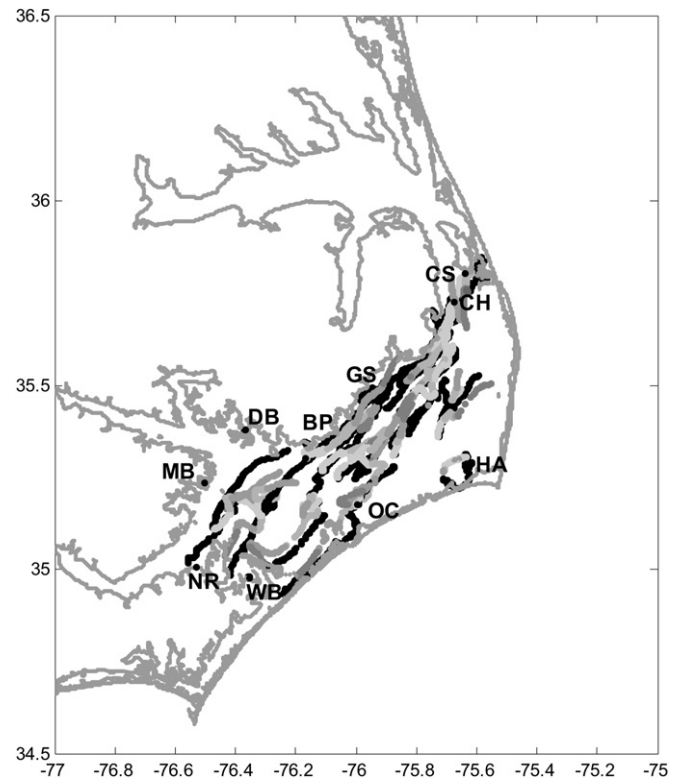


**Fig. 6.** Comparison of observed dispersal from 25 surface drifters (gray) and predicted dispersal from Particle-Tracking Model (black). Deployment details are listed in Table 2. For reference, Croatan Sound (CS), Crab Hole (CH), Gibbs Shoal (GS), Bluff Point (BP), Deep Bay (DB), Middle Bay (MB), Neuse River (NR), West Bay (WB), Ocracoke (OC), and Hatteras (HA) oyster reserves are shown. Drifter dispersal colors correspond to deployment duration, whereby color transitions from lightest to darkest gray from day 1–4, respectively. Highest cross-correlations among observed and predicted dispersal occur when dispersal overlaps.

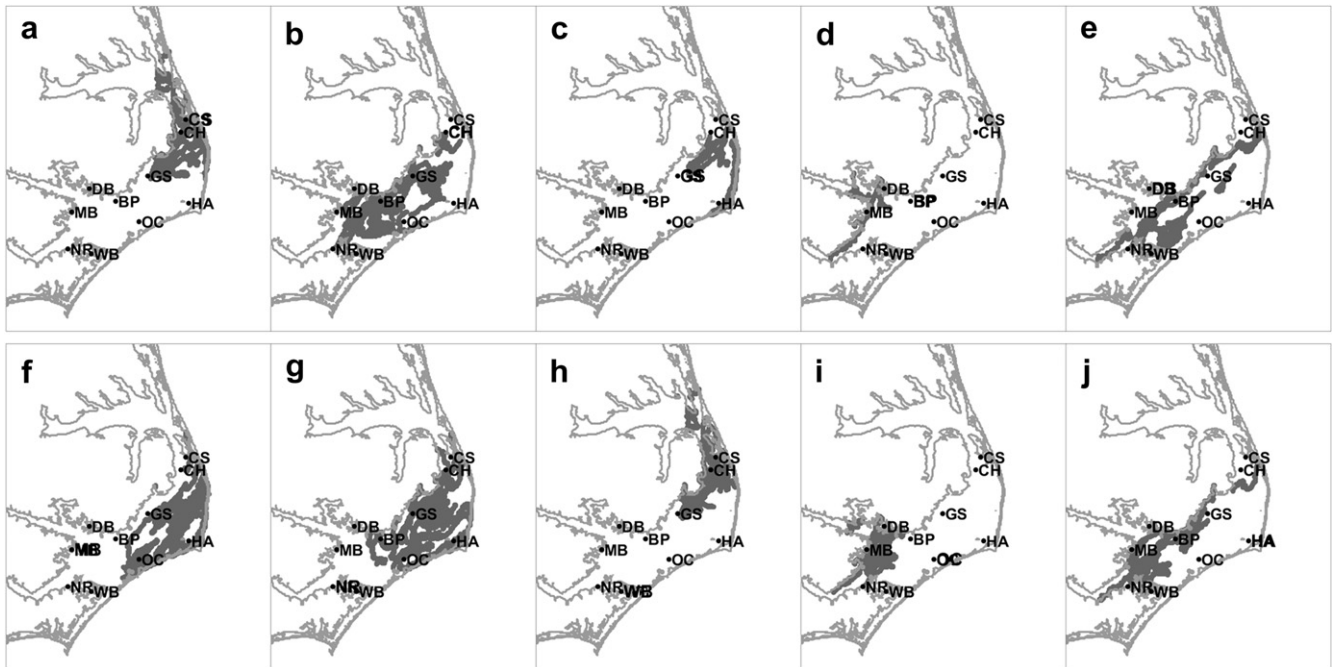


Fig. 7. Potential larval settlement areas in Pamlico Sound for virtual oyster larvae released from a) Croatan Sound, b) Crab Hole, c) Gibbs Shoal, d) Bluff Point, e) Deep Bay, f) Middle Bay, g) Neuse River, h) West Bay, i) Ocracoke, and j) Hatteras oyster reserves. Lines represent the final 7 days of particle dispersal where oysters are assumed competent to settle. Release reserves are denoted with bold lettering.

settlement areas for virtual larvae released from Deep Bay and Hatteras were located primarily along-shore in PS (Fig. 7e and j).

### 3.3.2. Potential connectivity among reserves

Potential oyster larval connectivity was not uniform among broodstock reserves in PS. The reserves with the largest potential settlement areas, Bluff Point and Gibbs Shoal, produced the greatest number of connections to neighboring reserves, with connectivity scores of 65 (out of 100) and 59, respectively (Table 3). Middle Bay, Deep Bay and Hatteras produced the fewest possible connections, a score of 20 or less (Table 3). All reserves, however, potentially self-recruit oyster larvae as indicated by a score of “10” in the cells along the main diagonal of the connectivity matrix (Table 3). Neuse River was an exception to this rule and scored a nine for self-recruitment since particles came within  $0.01^\circ$  but did not re-enter the reserve. Summing the columns of the connectivity matrix (Table 3) to interpret the relative degree of connectivity between all the reserves within the network and a given reserve, indicated that Crab Hole and Gibbs Shoal potentially received the greatest supply of larvae from other reserves, with percent connectivity scores of 56. Conversely, Croatan Sound, though proximal to Crab Hole, scored 38.

Of the 100 possible connections, 24 were present. Eight of the 10 reserves provided  $\geq$  one inter-reserve connection, with 4 being the most. Self-recruitment occurred at all but one reserve. Although reserve boundaries were expanded by  $0.01^\circ$ ,  $0.02^\circ$ , and  $0.03^\circ$  (about 1 km, 2 km, and 3 km respectively), the number of inter-reserve connections and self-recruitment increased by 10, 12, and 13, respectively. Thus, increasing reserve size disproportionately increased reserve connectivity.

## 4. Discussion

A 3D numerical hydrodynamic model (ADCIRC) reliably predicted variation in estuarine current velocities over space and time in PS, especially currents near-surface. A PTM, using predicted

currents, also reliably simulated trajectories of surface drifters under varying wind regimes, thereby providing confidence in qualitative predictions of dispersal of virtual larvae, and potential larval connectivity among no-take oyster reserves in PS. From a management perspective, reserves where larvae are spread and transported to vast regions may be particularly desirable. If so, the reserves located at Gibbs Shoal and Bluff Point should be a management (e.g., stock enhancement) priority. Potential oyster larval connectivity was not uniform among broodstock reserves in PS; connectivity from the natal reserve to reserves within the network (including self-recruitment) ranged from 10 to 65. All reserves, with the exception of Middle Bay and Hatteras, provided one or more direct connections (i.e., connectivity = 10; Table 3) to reserves within the network. Moreover, all reserves potentially self-recruited. Reserves located at Gibbs Shoal and Bluff Point provided the most inter-reserve connections. The effects of reserve size on connectivity were most pronounced with relatively modest ( $0.01^\circ$ )

Table 3

Connectivity matrix. Potential larval connectivity between natal reserves (rows) and settlement reserves (columns). Score of 10 indicates direct connectivity. Scores of 9, 8, and 7 indicate potential settlement areas measured within  $0.02^\circ$ ,  $0.03^\circ$  and  $0.04^\circ$  latitude/longitude of reserve boundaries, respectively. Zeros indicate no potential settlement areas within  $0.04^\circ$  ( $\sim 4$  km) of a reserve boundary. Self-recruitment is indicated by the gray-shaded cells along the main diagonal of the connectivity matrix.

		CS	CH	GS	BP	DB	MB	NR	WB	OC	HA	Total
Croatan Sound	CS	10	10	9	0	0	0	0	0	0	0	29
Crab Hole	CH	10	10	9	0	0	0	0	0	0	0	29
Gibbs Shoal	GS	9	10	10	10	0	0	0	0	10	10	59
Bluff Point	BP	0	10	10	10	0	8	9	10	8	0	65
Deep Bay	DB	0	0	0	0	10	10	0	0	0	0	20
Middle Bay	MB	0	0	0	0	0	10	0	0	0	0	10
Neuse River	NR	0	0	9	10	0	10	9	10	0	0	48
West Bay	WB	0	0	9	10	0	0	9	10	0	0	38
Ocracoke	OC	9	9	0	0	0	0	0	0	10	10	38
Hatteras	HA	0	7	0	0	0	0	0	0	0	10	17
Total		38	56	56	40	10	38	27	30	28	30	

size increases. Increasing reserve size resulted in reserves located at Bluff Point, West Bay, and Ocracoke receiving the most additional connections, which suggests that these two reserves should receive priority for reserve expansion. Spatial variation in the degree of potential oyster larval connectivity in PS, combined with spatio-temporal variation in demographic rates of oysters (e.g., fecundity, settlement, growth, survival) in PS (Mroch et al., in review, Puckett and Eggleston, in review), provides strong evidence for an oyster metapopulation and possibly source-sink dynamics within the network of no-take oyster reserves in PS (Eggleston, 1999; Lipcius et al., 2008). Recalling that a metapopulation is discrete, but connected populations characterized by spatially dynamic demographics, it appears that the oyster broodstock reserves in PS are particularly amenable to testing metapopulation and source-sink concepts because of: (1) the presence of discrete broodstock reserves that are separated by ~10–125 km, (2) spatial variation in the timing of spawning (Eggleston and Ballance, 2007), (3) spatial variation in oyster demographic rates such as fecundity, growth and survival (Mroch et al. in review, Puckett and Eggleston, in review), and (4) variation in potential larval connectivity (this study).

#### 4.1. Efficacy of ADCIRC hydrodynamic model in predicting current velocities

We tested the efficacy of 2D versus 3D ADCIRC hydrodynamic models in predicting observed current velocities across a wide range of wind conditions and two geographically distinct areas in PS. Moored ADCP instruments, which collected Eulerian data on vertical distribution of velocities, were deployed in areas of PS where the model's predictive abilities were presumed to be limited, for instance near complex terrain features such as Bluff Shoals, as well as near inlets. The 3D model generated more accurate predictions of surface velocities, particularly the magnitude of surface velocity, than the 2D model. Current velocities predicted with the 2D ADCIRC model were, in general, an order of magnitude slower than observed currents, whereas velocities predicted with the 3D model were in good agreement with the observations (Figs. 3–5). Similarly, observations of currents in Beaufort Inlet, NC south of PS, collected with a combination of current meters and ADCP transects agreed well with 2D ADCIRC model predictions, especially in capturing both amplitude and phase of tidal constituents, and direction of flow, but under-predicted maximum current flux by as much as 50% (Luettich et al., 1999). Near-surface observations of currents in the northern region of PS during the fall recruitment period for blue crab (*Callinectes sapidus*) megalopae and early juveniles using S4 current meters were well-predicted by ADCIRC with statistical correlations between 0.4 and 0.9 (Reyns et al., 2006, 2007). Other studies have validated ADCIRC model predictions, and generally found that the numerical predictions agreed well with observations (Luettich et al., 2002; Westerink et al., 2008).

#### 4.2. Efficacy of PTM in predicting oyster larval dispersal

We tested the ability of the PTM to replicate observed Eulerian and Lagrangian velocities in a challenging environment to model, the wind-driven micro-tidal currents of PS. Additionally, we tested the PTM across a large spatial range, nearly the entire PS, using ADCIRC vector fields driven by spatially consistent winds. A collection of drifter observations were used to validate predictions from the PTM, which was then used to predict potential larval paths. Through analysis of the observations and modeled flow-fields, several unique features were discovered in PS that have

implications for larval connectivity (see 4.3 Potential oyster larval settlement areas and connectivity among oyster reserves).

Drifters were deployed in other studies off the Southeast US Continental Shelf which provided estimates of the retentive characteristic of the Southeast US Continental Shelf and showed overall good agreement between numerical and observed drifter tracks with regression coefficients ( $R^2$ ) ranging from 0.48 to 0.89 (Edwards et al., 2006; Hare and Walsh, 2007). To date, no known published record exists of other drifter studies conducted within PS.

Weekly drifter releases were conducted across the northern and southern basins of PS during both the northeasterly and southwesterly wind regimes. Release sites were selected based on wind forecasts, southern release sites for southerly wind forecasts and northern release sites for northerly wind forecasts (Table 1 and Fig. 1). These release sites proved to be highly effective since drifters remained in PS during most deployments. On a few occasions, however, drifters deployed in the north exited the study area through Oregon Inlet and Croatan Sound. In the south, drifters exited PS through Neuse River, but not through Ocracoke Inlet. This only caused minor interruptions in the data collection (<2 d) and suggests oyster larvae could be exported from PS to the Atlantic Ocean under similar circumstances.

Surprisingly, the predicted dispersal of particles generated by the PTM were generally longer than the Lagrangian observations of surface drifters, despite the ADCIRC-predicted current velocities being less energetic than the Eulerian observations. The mechanisms causing this unexpected result are not entirely known, though it could be attributed to slip velocities in the drifters which were reported to be 1–3 cm s<sup>-1</sup> for the tri-star drogue configuration (Niiler et al., 1987, 1995; Geyer, 1988). When drifter velocities were compared to ADCP velocities for concurrent observations, however, mean velocities for both instruments were within 1 cm s<sup>-1</sup> of each other. Alternatively, the magnitude of the wind velocity and responding currents generally diminished near dawn and increased during afternoon hours, but this diurnal dynamic was not completely captured in the time-series predicted velocity plots, particularly the relaxation during early morning hours. By not including this morning relaxation, the dispersal of virtual particles could exceed that of drifter observations. Lastly, it is possible hydrodynamic features not visible in the observations, such as frontal boundaries, could have entrained drifters thereby slowing them down relative to predicted speeds and distances (e.g., Eggleston et al., 1998). A possible solution to this discrepancy between predicted and observed dispersal would be to create an interpolation of variable depth layers for the uppermost 1 m depth, particularly in shallower areas (<7 m deep) where layers are much less than 1 m. Observed dispersal could then be compared to dispersal predicted by velocities in the surface 1 m rather than the uppermost layer of the model. This was not performed because global velocities predicted in the numerical model decreased significantly below the uppermost depth layer.

#### 4.3. Potential oyster larval settlement areas and connectivity among oyster reserves

The present study provides evidence that circulation in PS can support an oyster metapopulation via larval connectivity of spatially-isolated broodstock reserves. For instance, the geometry of the narrow Croatan Sound connecting Pamlico Sound to Albemarle Sound (Fig. 1) could potentially facilitate oyster larval connectivity. During southwesterly winds, ADCIRC flow-fields indicated surface waters originating in PS were pushed north into Albemarle Sound via Croatan Sound, while the bottom layer produced a weak return flow to the south. This bi-layer circulation

continued until either the wind force decreased or the pressure gradient produced by the increased water depth exceeded the wind force. Once this balance of forces between the wind and the pressure gradient was interrupted, Croatan Sound acted like a *venturi* described by Bernoulli's Principle (Halliday and Resnick, 1960; Bernoulli, 1738) whereby water from Albemarle Sound flowed south out of Croatan Sound into PS creating a strong southward flow at all depths. Velocities measured by the ADCP at Crab Hole exceeded  $0.5 \text{ m s}^{-1}$ , and this event is referred to as the "Albemarle Flush" hereafter. Drifters caught in the Albemarle Flush traveled up-wind (i.e. to the south when the winds were blowing southwesterly). Mean velocities and principle components from the ADCP moored at Crab Hole were dominated by a southward component likely caused by the Albemarle Flush. This behavior observed by the drifters and ADCP at Crab Hole could not be explained until the Albemarle Flush was detected in the global velocities produced by the 3D ADCIRC model. Oyster larvae spawned from Croatan Sound or Crab Hole could be advected south toward Gibbs Shoal and Bluff Point during occurrences of the Albemarle Flush, thereby enhancing potential larval connectivity between these northern reserves and those located to the south when, during much of the spawning season, winds are predominantly southwesterly. Other mechanisms, such as underwater shoals, hydrodynamic isolation in bays and diminished strength in the nocturnal winds could promote self-recruitment.

#### 4.4. Assumptions and applications

Oyster larvae are known to migrate throughout the water column in an effort to track the halocline (Deksheniaks et al., 1996; North et al., 2008). In PS, however, the water column is generally well-mixed and often behaved as a single layer where profile observations were collected. Thus, we did not attempt to integrate oyster larval vertical migration behavior, nor ontogenetic changes in depth as oyster larvae mature, into the PTM in this study. We also did not integrate tides from the Atlantic Ocean into the PTM since the tidal influence on current velocities diminishes significantly with distance from the inlets (Pietrafesa et al., 1986; Luettich et al., 2002). It is possible that virtual particles, when not restricted to PS (i.e., hydrodynamically connected to the Atlantic Ocean), would exit PS into the Atlantic Ocean through Oregon, Hatteras or Ocracoke Inlets as demonstrated by the drifters. This research project focused on oysters whose larvae are spawned in PS and accepted this minor limitation since most oyster reserves are located away from inlets.

## 5. Conclusion

In conclusion, solving the larval dispersal challenge requires a diverse set of techniques, each with its own strengths and limitations for a given study system and spatiotemporal scale. These methods include field sampling of larvae and currents coupled with bio-physical modeling, drifters, and genetic or geochemical tagging (NSF, 2002). The results of this study validate existing tools and applications for studying larval dispersal in primarily wind-driven estuaries such as PS. For example, we demonstrated the efficacy of (1) ADCIRC in recreating 3D velocities in complex bathymetric and geo-morphological settings within a primarily wind-driven estuary, and (2) an ADCIRC-based PTM in recreating larval dispersal trajectories, which are critical in estimating larval connectivity among reserve networks. Testing and refinement of numerical hydrodynamic models, PTMs, and techniques for validating these predictions, such as bottom-moored ADCP and satellite drifters, will enhance decision support tools for improving the efficacy of reserve networks for marine habitat and fisheries management and restoration purposes.

## Acknowledgments

Financial support for this project was provided by the North Carolina Sea Grant College Program (Grants R/MRD-53 and R/MRD-56 to D. Eggleston), and the Blue Crab Advanced Research Consortium, Center of Marine Biotechnology, University of Maryland to D. Eggleston. We thank C. Cudaback for her help in initiating the drifter aspect of this study. The authors thank Steve Rebach and Bob Hines for their administration of the NC Sea Grant component of this project. The authors would also like to acknowledge the NC Division of Marine Fisheries and the US Coast Guard Auxiliary for their assistance releasing and retrieving drifters, the Nature Conservancy for purchase of batteries, and Pacific Gyre for technical assistance, maintenance and repairs of drifters.

## References

- Beck, M.W., Brumbaugh, B.D., Airoldi, L., Carranza, A., Coen, L.D., Crawford, C., Defeo, O., Edgar, G.J., Hancock, B., Kay, M.C., Lenihan, H.S., Luckenbach, M.W., Toropova, C.L., Zhang, G., Guo, X., 2011. Oyster reefs at risk and recommendations for conservation, restoration, and management. *BioScience* 61 (2), 107–116.
- Becker, B.J., Levin, L.A., Fodrie, F.J., McMillan, P.A., 2007. Complex larval connectivity patterns among marine invertebrate populations. *National Academy of Science* 104 (9), 3267–3272.
- Bernoulli, D.J., 1738. *Hydrodynamica, sive, De viribus et motibus fluidorum commentarii: opus academicum ab auctore, dum Petropoli ageret, congestum. Sumpibus Johannis Reinholdi Dulseckeri*, p 304.
- Briers, R.A., 2002. Incorporating connectivity into reserve selection procedures. *Biological Conservation* 103 (1), 77–83.
- Burkenroad, M.D., 1931. Sex in the Louisiana oyster *Ostrea virginica*. *Science* 74 (1907), 71–72.
- Cowen, R.K., Gawarkiewicz, G., Pineda, J., Thorrold, S.R., Werner, F.E., 2007. Population connectivity in marine systems: an overview. *Oceanography* 20 (3), 14–21.
- Cowen, R.K., Paris, C.B., Srinivasan, A., 2006. Scaling of connectivity in marine populations. *Science* 311, 522–527.
- Cowen, R.K., Sponaugle, S., 2009. Larval dispersal and marine population connectivity. *Annual Review of Marine Science* 1, 443–466.
- Cudney-Bueno, R., Lavin, M.F., Marinone, S.G., Raimondi, P.T., Shaw, W.W., 2009. Rapid effects of marine reserves via larval dispersal. *PLoS ONE* 4, 1–7.
- Deksheniaks, M., Hofmann, E., Klinck, J., Powell, E., 1996. Modeling the vertical distribution of oyster larvae in response to environmental conditions. *Marine Ecology Progress Series* 136, 97–110.
- Deksheniaks, M., Hofmann, E., Klinck, J., Powell, E., 1993. Environmental effects on the growth and development of Eastern Oyster, *Crassostrea Virginica* (Gmelin, 1971), larvae: a model study. *Journal of Shellfish Research* 12, 241–254.
- Doble, M.J., Wadhams, P., 2006. Dynamical contrasts between pancake and pack ice, investigated with a drifting buoy array. *Journal of Geophysical Research* 3 (C11S24), 11. doi:10.1029/2005JC003320.
- Edwards, K.P., Hare, J.A., Werner, F.E., Blanton, B.O., 2006. Lagrangian circulation on the Southeast US Continental Shelf: implications for larval dispersal and retention. *Continental Shelf Research* 26, 1375–1394.
- Eggleston, D.B., Reynolds, N.B., Etherington, L.L., Plaia, G.R., Xie, L., 2010. Tropical storm and environmental forcing on regional blue crab (*Callinectes sapidus*) settlement. *Fisheries Oceanography* 19, 89–106.
- Eggleston, D.B., 1999. Application of landscape ecological principles to oyster reef habitat restoration. In: Luckenbach, M.W., Mann, R., Wesson, J.A. (Eds.), *Oyster Reef Habitat Restoration: a Synopsis and Synthesis of Approaches*. Virginia Institute of Marine Science Press, pp. 213–277.
- Eggleston, D.B., Armstrong, D.A., Elis, W.E., Patton, W.S., 1998. Estuarine fronts as conduits for larval transport: hydrodynamic and spatial distribution of Dungeness crab postlarvae. *Marine Ecology Progress Series* 164, 73–82.
- Eggleston, D.B., Ballance, E., 2007. Oyster mapping and metapopulation dynamics in Pamlico Sound, Final Report for FRG Project 06-EP-03, p. 33.
- Figueira, W.F., Crowder, L.B., 2006. Defining patch contribution in source-sink metapopulations: the importance of including dispersal and its relevance to marine systems. *Population Ecology* 48, 215–224.
- Fodrie, F.J., Becker, B.J., Levin, L.A., Gruenthal, K., McMillan, P.A., 2011. Connectivity clues from short-term variability in settlement and geochemical tags of mytilid mussels. *Journal of Sea Research* 65, 141–150.
- Gaines, S.D., White, C., Carr, M.H., Palumbi, S.R., 2010. Designing marine reserve networks for both conservation and fisheries management. *Proceedings of the National Academy of Sciences* 107, 18286–18293.
- Geyer, W.R., 1988. Field calibration of mixed-layer drifters. *Journal of Atmospheric and Oceanic Technology* 6, 333–342.
- Halliday, D., Resnick, R., 1960. *Physics*. John Wiley & Sons, Inc, p. 1025.
- Hanski, I., 1998. Metapopulation dynamics. *Nature* 396, 41–49.

- Hare, J.A., Walsh, H.J., 2007. Planktonic linkages among marine protected areas on the south Florida and southeast United States continental shelves. *Canadian Journal of Fisheries and Aquatic Sciences* 64, 1234–1247.
- Levins, R., 1969. Some demographic and genetic consequences of environmental heterogeneity for biological control. *Bulletin of the Entomology Society of America* 15, 237–240.
- Lin, J., Xie, L., Pietrafesa, L.J., Ramus, J.S., Paerl, H.W., 2007. Water quality gradients across Albemarle-Pamlico Estuarine System: seasonal variations and model applications. *Journal of Coastal Research* 23, 213–229.
- Lipcius, R.N., Eggleston, D.B., Schreiber, S.J., Seitz, R.D., Shen, J., Sisson, M., Stockhausen, W.T., Wang, H.V., 2008. Importance of metapopulation connectivity to restocking and restoration of marine species. *Reviews in Fisheries Science* 16 (1–3), 101–110.
- Luettich, R.A., Carr, S., Reynolds-Fleming, J., Fulcher, C.W., McNinch, J., 2002. Semi-diurnal seiche in a shallow, micro-tidal lagoonal estuary. *Continental Shelf Research* 22, 1669–1681.
- Luettich, R.A., Hensch, J.L., Fulcher, C.W., Werner, F.E., Blanton, B.O., Churchill, J.H., 1999. Barotropic tidal and wind-driven larval transport in the vicinity of a barrier island inlet. *Fisheries Oceanography* 8, 190–209.
- Luettich, R.A., Westerink, J.J., 2004. Formulation and Numerical Implementation of the 2D/3D ADCIRC Finite Element Model Version 44.xx, p. 74.
- Luettich, R.A., Westerink, J.J., Scheffner, N.W., 1992. ADCIRC: an advanced three-dimensional circulation model for shelves coasts and estuaries, report 1: theory and methodology of ADCIRC-2DDI and ADCIRC-3DL, Dredging Research Program Technical Report DRP-92–96. U.S. Army Engineers Waterways Experiment Station, Vicksburg, MS, p. 137.
- Mroch, R., 2009. Spatiotemporal variation in broodstock reserve fecundity. M.S. thesis, NC State University, Raleigh, NC 27695 USA, p. 70.
- Niiler, P.P., Sybrandt, A.S., Bi, K., Poulain, P.M., Bitterman, D., 1995. Measurements of the water-following capability of holey-sock and TRISTAR drifters. *Deep-Sea Research* 42, 1951–1964.
- Niiler, P.P., Davis, R.E., White, J.J., 1987. Water-following characteristics of a mixed layer drifter. *Deep-Sea Research* 34, 1867–1881.
- North, E.W., Schlag, Z., Hood, R.R., Li, M., Zhong, L., Gross, T., Kennedy, V.S., 2008. Vertical swimming behavior influences the dispersal of simulated oyster larvae in a coupled particle-tracking and hydrodynamic model of Chesapeake Bay. *Marine Ecology Progress Series* 359, 99–115.
- NSF (National Science Foundation), 2002. Population connectivity in marine systems. In: Workshop Convenors, Cowen, R.K., Gawarkiewicz, G., Pineda, J., Thorrold, S., Werner, F. (Eds.), Report of a workshop to develop science recommendations for the National Science Foundation. November 4–6, 2002. Durango, Colorado.
- Pietrafesa, L.J., Janowitz, G.S., 1988. Physical oceanographic processes affecting larval transport around and through North Carolina inlets. *American Fisheries Society Symposium* 3, 34–50.
- Pietrafesa, L.J., Janowitz, G.S., Chao, T.-Y., Weisburg, R.H., Askari, F., Noble, E., 1986. The Physical Oceanography of Pamlico Sound. Report UNC-SG-WP-86-5. Sea Grant Program of the University of North Carolina, Raleigh, NC, p. 126.
- Powers, S.P., Peterson, C.H., Grabowski, J.H., Lenihan, H.S., 2009. Success of constructed oyster reefs in no-harvest sanctuaries: implications for restoration. *Marine Ecology Progress Series* 389, 159–170.
- Puckett, B. J. and Eggleston, D. B. Oyster dynamics in a network of no-take reserves. I. Recruitment, growth, survival, and density dependence. *Marine Ecology Progress Series*, in review.
- Reynolds-Fleming, J.V., Luettich, R.A., 2004. Wind-driven lateral variability in a partially mixed estuary. *Estuarine Coastal and Shelf Science* 60, 395–407.
- Reyns, N.B., Eggleston, D.B., Luettich, R.A., 2006. Secondary dispersal of early juvenile blue crabs within a wind-driven estuary. *Limnology and Oceanography* 51, 1982–1995.
- Reyns, N.B., Eggleston, D.B., Luettich, R.A., 2007. Dispersal dynamics of post-larval blue crabs, *Callinectes sapidus*, within a wind-driven estuary. *Fisheries Oceanography* 16 (3), 257–272.
- Roberts, C.M., Branch, G., Bustamante, R.H., Castilla, J.C., Dugan, J., Halpern, B.S., Lafferty, K.D., Leslie, H., Lubchenco, J., McArdle, D., Ruckelshaus, M., Warner, R.R., 2003. Applications of ecological criteria in selecting marine reserves and developing reserve networks. *Ecological Applications* 13, S215–S228.
- Schulte, D.M., Burke, R.P., Lipcius, R.N., 2009. Unprecedented restoration of a native oyster metapopulation. *Science* 325, 1124–1127.
- Spalding, M.D., Fish, L., Wood, L.J., 2008. Toward representative protection of the world's coasts and oceans – progress, gaps, and opportunities. *Conservation Letters* 1, 217–226.
- Stanley, J.G., Sellers, M.A., 1986. Species Profiles: Life Histories and Environmental Requirements of Coastal Fishes and Invertebrates (Gulf of Mexico): American Oyster, vol. 82, U.S. Fish and Wildlife Service Biological Report. (11.64.) p. 25.
- Steneck, R.S., 2006. Staying connected in a turbulent world. *Ecology* 311, 480–481.
- Westerink, J.J., Luettich, R.A., Feyen, J.C., Atkinson, J.H., Dawson, C., Roberts, H.J., Powell, M.D., Dunion, J.P., Kubatko, E.J., Pourtaheri, H., 2008. A basin- to channel-scale unstructured grid hurricane storm surge model applied to Southern Louisiana. *Monthly Weather Review* 136, 833–864.
- Xie, L., Eggleston, D.B., 1999. Computer simulation of wind-induced estuarine circulation patterns and estuary-shelf exchange process: the potential role of wind forcing on larval transport. *Estuarine Coastal and Shelf Science* 49, 221–234.